

Trends in **Applied Sciences** Research

ISSN 1819-3579



Trends in Applied Sciences Research 9 (8): 461-471, 2014 ISSN 1819-3579 / DOI: 10.3923/tasr.2014.461.471 © 2014 Academic Journals Inc.

A Chirp Spread Spectrum FSK IR-UWB Receiver

Hatem Trabelsi, Imen Barraj and Mohamed Masmoudi

Laboratory of Micro-Electro Thermal Systems (METS), National Engineers School of Sfax, University of Sfax, B.P. 1173, Sfax 3038, Tunisia

Corresponding Author: Hatem Trabelsi, Laboratory of Micro-Electro Thermal Systems (METS), National Engineers School of Sfax, University of Sfax, B.P. 1173, Sfax 3038, Tunisia Tel: (+216) 74 274 088 Fax: (+216) 74 677 657

ABSTRACT

A chirp spread spectrum FSK impulse radio ultra-wideband (IR-UWB) receiver for low data rate, wireless sensor device, operating in the 3-5 GHz (UWB) is described in this study. Chirped spread spectrum FSK modulation enables direct conversion technique with non coherent demodulator which simplifies the receiver architecture. Two sub-bands frequencies are used to encode the binary data. A variable bandwidth low pass filter is used to pass the desired sub-band and eliminate in-band interference in order to improve receiver sensitivity. More than 65 dB of side lobe rejection is achieved at receiver output. The various blocks parameters of the receiver are simulated and optimized to meet receiver specifications. The in-band receiver conversion gain is 99 dB while the NF is 5.4 dB only. The receiver realizes a sensitivity of -86 dBm, an output power of 13 dBm and an IIP3 of -8.8 dBm.

Key words: IR-UWB, chirp spread spectrum, FSK, receiver front end

INTRODUCTION

The recent advances in microelectronics and Micro Electro Mechanical Systems (MEMS) have produced miniaturized, low-power and inexpensive components for numberless applications like micro sensing and RF transceiver (Padmanabhan *et al.*, 1997; Abidi *et al.*, 2000).

Various applications of sensor networks around different fields have emerged including healthcare and motion detection (Culler *et al.*, 2004; Lorincz *et al.*, 2004).

However, because of their characteristics (energy constraint, reduced capacity of nodes, large number of sensors), reducing the power consumption of these sensors is a scientific challenge.

The transceiver is the element consuming more energy in wireless sensors. For this reason, many studies are interested on power consumption of radiofrequency part "RF front end" by choosing the most suitable architecture for RF wireless sensors, modulation technique and transistor level optimization of the various blocks of the transceiver.

Ultra-wideband (UWB) has never been as popular as it is now. Numerous researches have concentrated on the UWB technology and its applications. This technology opens a new era of practical applications in home/office/factory automation and wireless body area network (Paulson et al., 2005; Saputra and Long, 2011; Diao et al., 2009). Because of the wide frequency content of the UWB signal, it can penetrate in biological materials such as skin, fat and other organic tissues and the reflection from the internal organs provides means to monitor vital signs (Staderini, 2002; Bilich, 2006).

The goal of this study is to design a low-complexity chirped spread spectrum FSK IR-UWB receiver for low data rate, short range application, operating in the 3-5 GHz ultra-wideband (UWB) for medical wireless sensor application which is competitive in terms of power

consumption. The receiver should communicate a maximum data rate of 3.2 Mbps with a pulse width of 75 nsec and a chirped frequency range of 500 MHz.

Parameters for each block of the receiver chain should be optimized so they meet receiver specifications.

Typical impulse radio UWB (IR-UWB) transceiver uses Gaussian pulses that are scaled to fit the desired bandwidth by varying the pulse width and amplitude (Diao et al., 2009). For low data rate UWB wireless sensor application we need to use narrow width pulses with large peak amplitude to obtain the desired UWB spectrum. These pulses cannot be easily generated using advanced CMOS technologies which are not amenable to large voltage swings due to lower supply. That is why we use a new form of modulation for IR-UWB transmission based on chirped spread spectrum FSK technique.

Chirped Spread Spectrum (CSS) pulse is a spread spectrum system which can generate a sinusoidal signal whose frequency increases or decreases linearly over a certain amount of time. The CSS solution can be used in secured medical applications as it is very difficult to detect and intercept when operating at low power. This technique may also be used within wireless devices moving at high speeds, alarm systems for predicting vehicles' collision and vehicle-to-vehicle communication.

In the traditional 2-FSK case, data bits are assigned tow fixed single tone carriers but in the proposed modulation scheme the '1's and '0's are assigned fixed sub-bands. These sub-bands are 3.2-3.7 GHz for data bit '0' and 4.0-4.5 GHz for data bit '1' and are denoted as SUBAND1 and SUBAND2 in the following analysis. The Federal Communications Committee (FCC) mask restricts the UWB emission power being under -41.3 dBm/MHz in the ranges of 3.1-10.6 GHz to reduce the potential interferences to existing applications (IEEE, 2007). In order to meet FCC mask requirements with conventional modulation schemes like OOK and PPM, high-swing Gaussian pulses requiring power hungry hardware for detection and synchronization are required (Barras et al., 2006). However, in the proposed design each sub band FSK pulse occupies 500 MHz of bandwidth which greatly relaxes the constraints on pulse width and swing to be employed while still retaining good overall mask occupancy.

MATERIALS AND METHODS

The receiver architecture is shown in Fig. 1. Direct conversion architecture is adopted because it eliminates the image-reject filter and other IF components, enabling a monolithic transceiver.

Pass band filtering provided by both antenna and LNA can attenuate the out-of-band signals at the receiver input. Therefore, RF band pass filter will not be used in this design. The received signal is first amplified with a Low Noise Amplifier (LNA) then down converted with the mixers using the quadrature sinusoidal tones produced by a quadrature Voltage Controlled Oscillator (VCO). A DAC is used to generate the control voltage for the VCO. The DAC should be able to produce the control voltages required so that the VCO frequency can be toggled over its entire tuning range. Steps of 30 MHz will be used to shift the LO frequency for good sensitivity (and hence energy detection) and to be able to shift the LO in case of interferer. A variable bandwidth low pass filter, in each path, passes only the selected down-converted sub-band signal and suppresses the other sub-band. Then amplifier with gain control is applied in order to achieve the sufficient dynamic range. Finally, non coherent sub bands FSK demodulator will retrieve the digital transmitted data.

Advanced Design System (ADS) tool was used to simulate the receiver. The aim of this simulation is to determine the optimized receiver blocks parameters that meet the overall wireless sensor specifications. Figure 2 shows the schematic diagram, used for simulation with

Trends Applied Sci. Res., 9 (8): 461-471, 2014

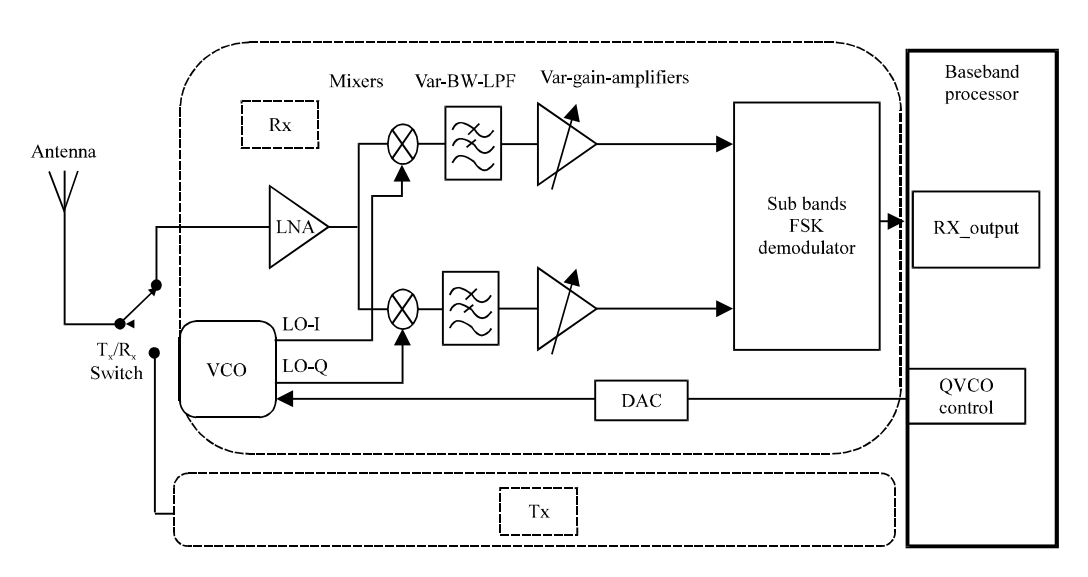


Fig. 1: Receiver architecture

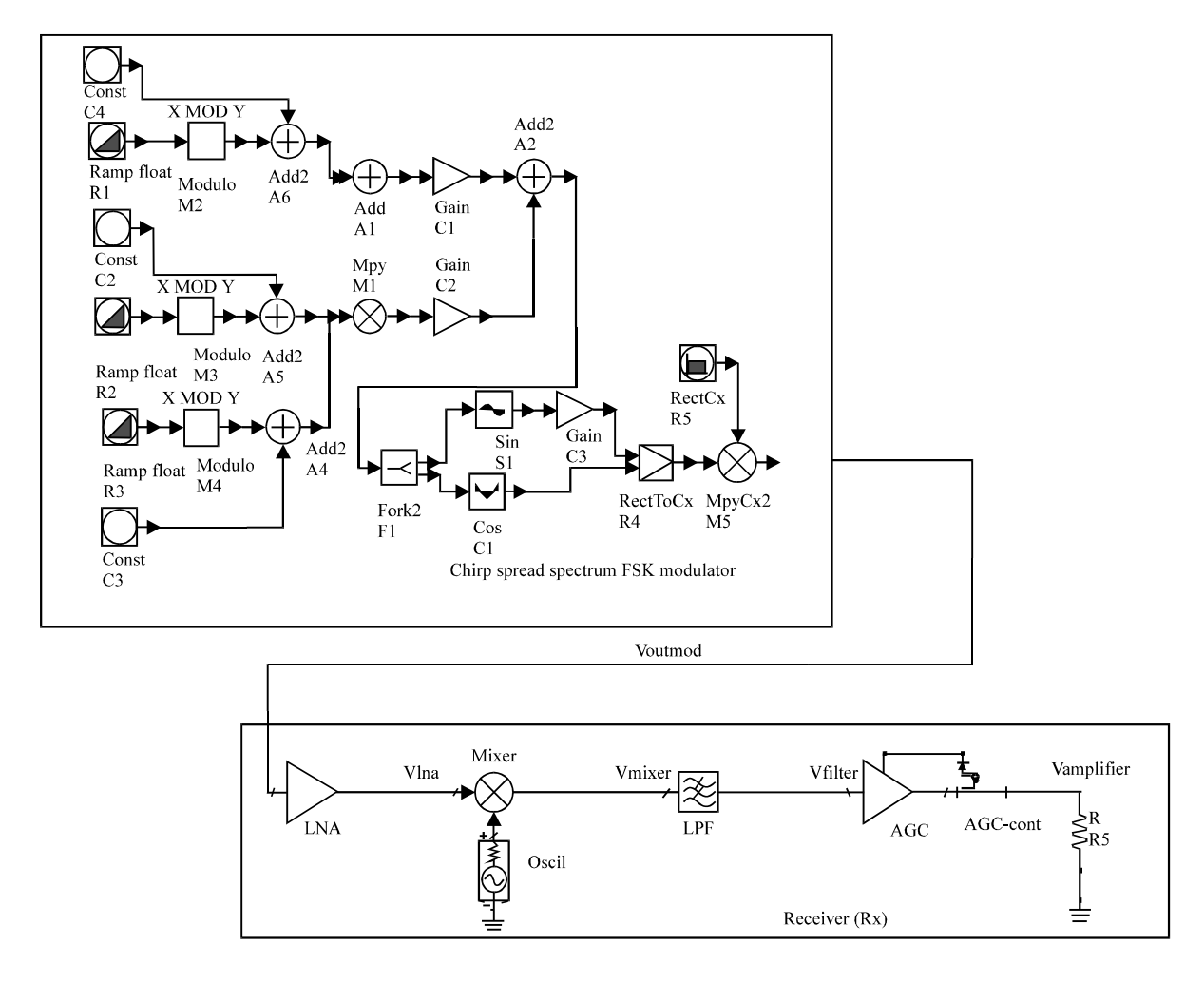


Fig. 2: Schematic diagram used for receiver simulation

digital chirp spread spectrum FSK modulator and receiver chain. The chirp value represents the amount of frequency shift over the full, extended pulse width which is 500 MHz. Voutmod is the dual band FSK chirped signal.

The modulator will send SUBAND1 signal in case of data bit '0' and SUBAND2 signal in case of data bit '1'. The target Pulse Repetition Frequency (PRF) is 3.2 Mbps.

RESULTS

Harmonic balance simulation: A harmonic balance simulation was conducted on ADS tool to evaluate receiver performance for both minimum and maximum receiver input power level. Figure 3 shows SUBAND1 chirped spread spectrum signal, LNA output, mixer output, receiver output and Tx binary data in time domain for a pulse width of 75 ns, a PRF of 3.2 MHz and a receiver maximum input power level of -14 dBm. Figure 4 shows FSK SUBAND1 (Voutmod), LNA output (Vlna), mixer output (Vmixer) and receiver output (Receiver_out) in frequency domain for a receiver input power level of -14 dBm. Figure 5 shows Power Spectral Density (PSD) at each node for a receiver sensitivity level of -86 dBm.

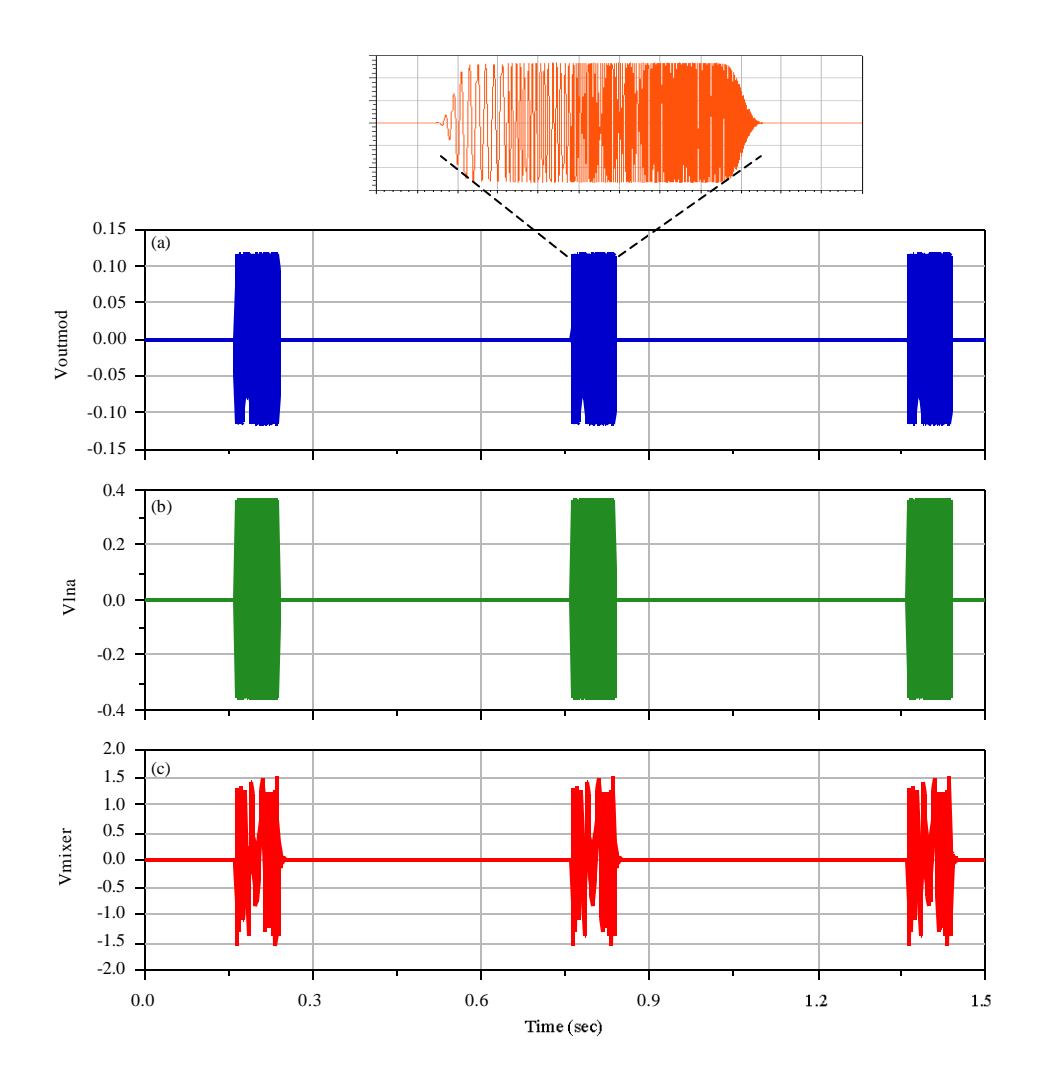


Fig. 3(a-e): Continue

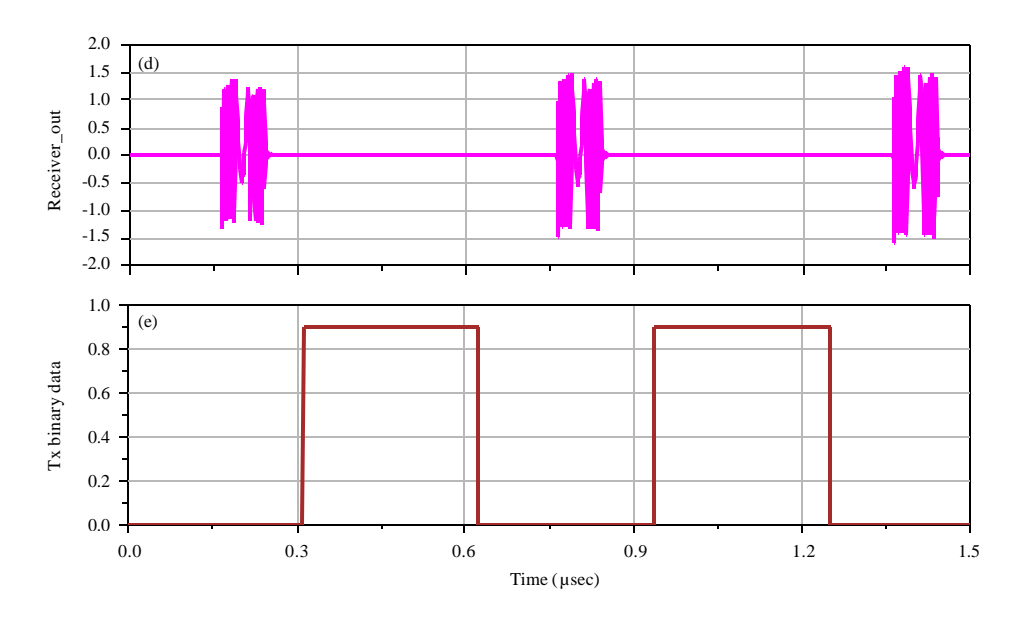


Fig. 3(a-e): Time representation of (a) SUBAND1 signal, (b) LNA output signal, (c) Mixer output signal, (d) Receiver output signal and (e) Transmitted binary data for $t_p = 75$ nsec, PRF = 3.2 MHz and a receiver input power level of -14 dBm

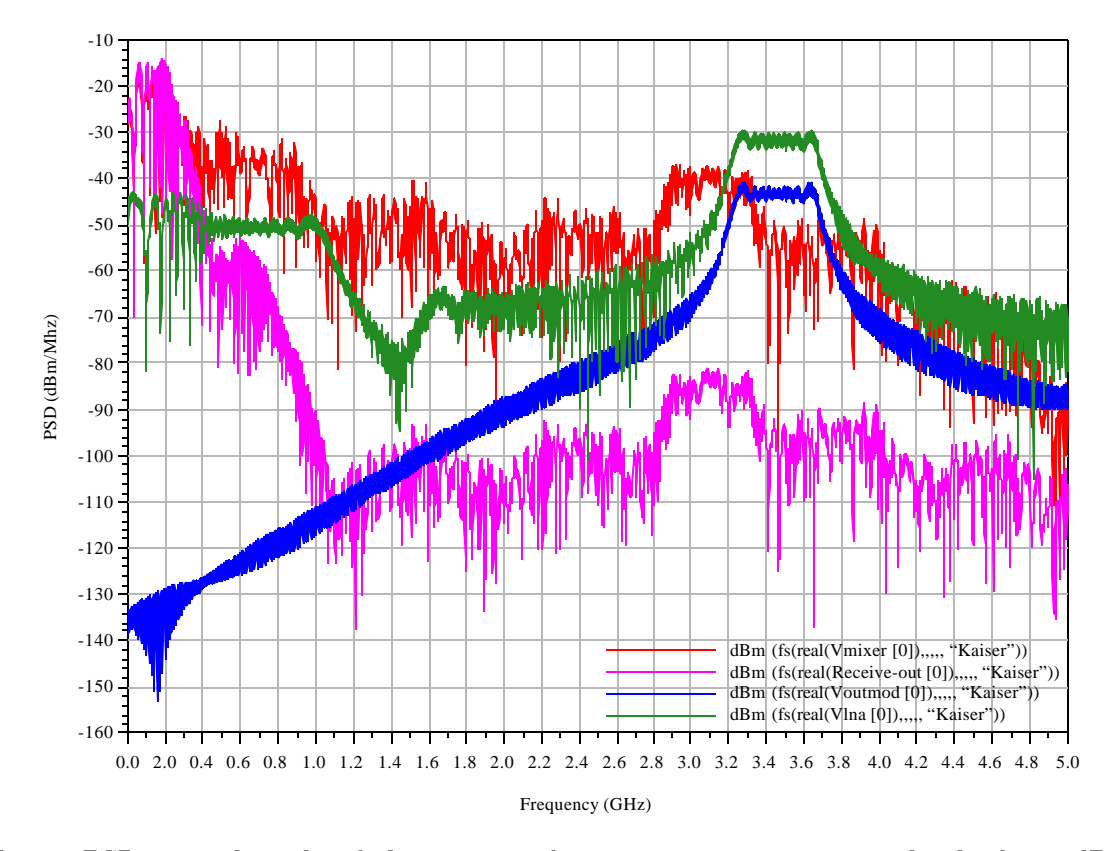


Fig. 4: PSD at each node of the receiver for a receiver input power level of -14 dBm, $t_p = 75 \; \mathrm{nsec}$ and PRF = 3.2 MHz

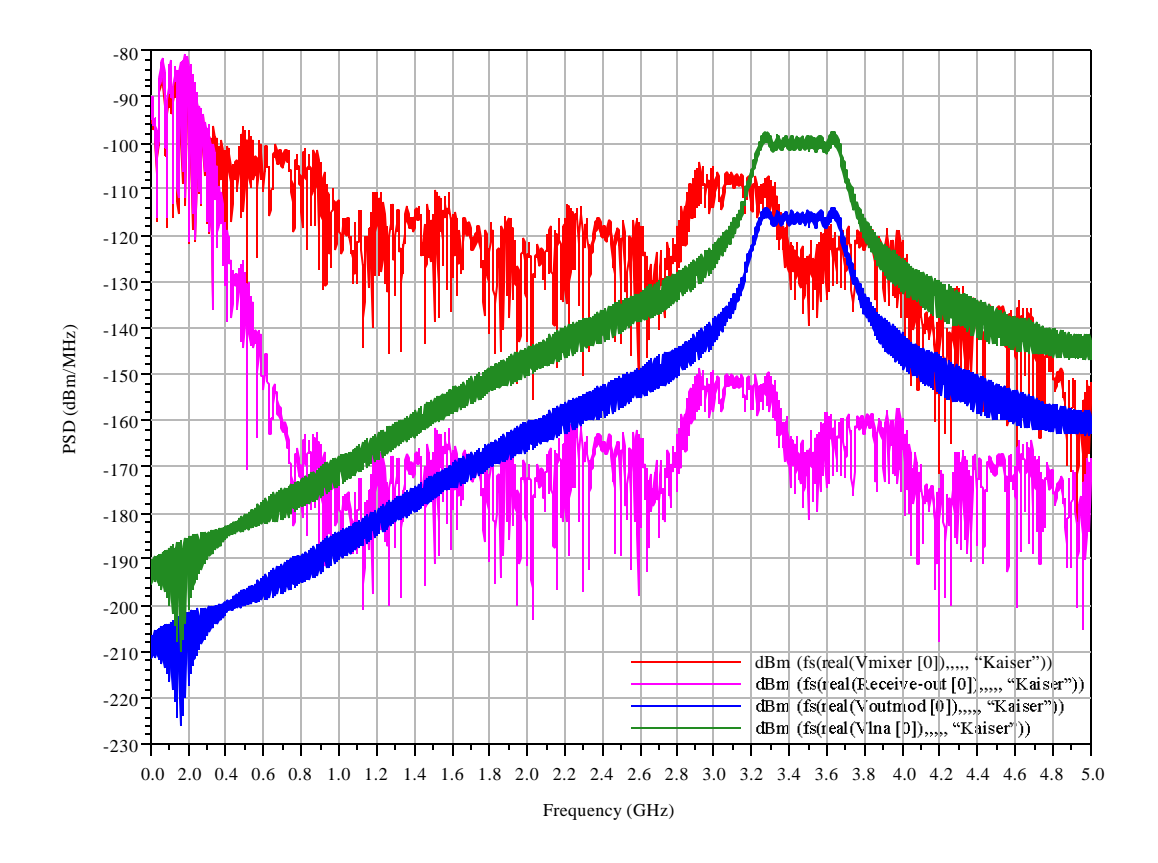


Fig. 5: PSD at each node of the receiver for a receiver sensitivity level of -86 dBm, $t_p = 75$ ns and PRF = 3.2 MHz

Variable bandwidth low pass filter: The Low Pass Filter (LPF) should have a large variable bandwidth and a sharp roll-off for maximum stop-band attenuation so the interference is greatly attenuated. An elliptic 5th order, sharp roll-off filter with 2 dB insertion loss and 65 dB rejection has been adopted.

Figure 6 shows that the LPF has an effective tuning range of 40-300 MHz in order to suppress any in-band narrowband interferers.

Budget simulation: For a maximum receiver input power of -14 dBm, the simulation shows a cascaded gain of 26.9 dB (Fig. 7a), a cascaded output power of 13 dBm (Fig. 7b) and a cascaded noise figure of about 5.4 dB (Fig. 7c). Figure 8 shows simulation results for a receiver sensitivity power of -86 dBm. The cascaded gain is now 99 dB (Fig. 8a) while the receiver maintains the same cascaded output power and noise figure as shown in Fig. 8b and c, respectively.

Figure 7d indicates that the receiver achieves a 1 dB compression point of -18.3 dBm and an IIP3 of -8.8 dBm which meet receiver specification.

Table 1 summarizes the overall simulated performances of the receiver and presents optimized circuits blocks requirements of the receiver front-end that meet overall UWB wireless sensor specifications.

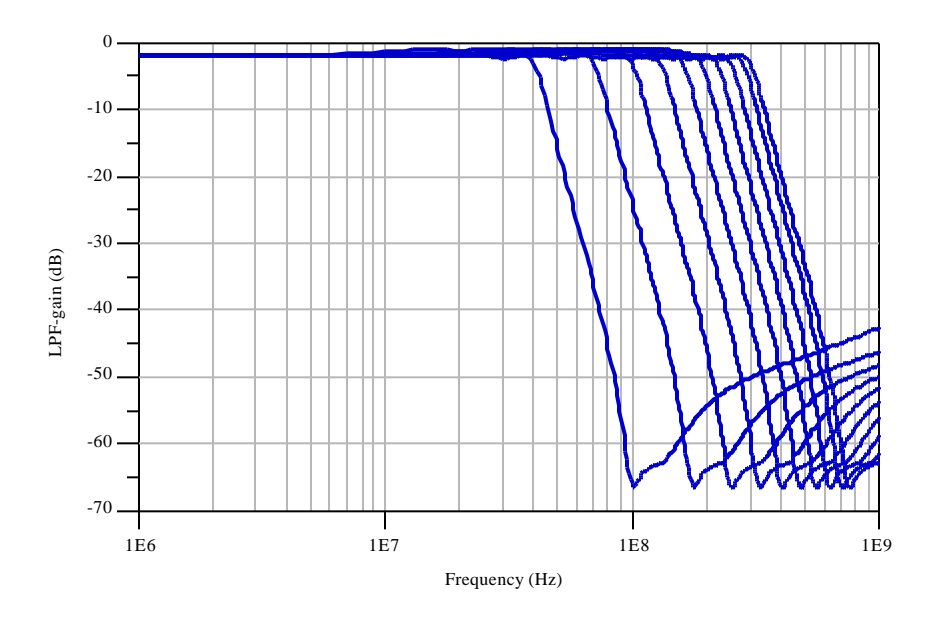


Fig. 6: Simulated frequency response of the variable bandwidth LPF

Table 1: Receiver performance summary and circuit blocks requirements

Receiver performance						
		Receiver blocks requirements				
IR-UWB	SUBAND 1 (3.2-3.7 Ghz)					
3-5 GHz	SUBAND 2 (4.0-4.5 GHz)	LNA	Mixer	Var-BW-LPF	VG-Amplifier	
Noise figure	5.4 dB	S21 = 18 dB	Con gain = 7 dB	Fpass = 40-300 MHz	Max_con gain = 80 dB	
Gain	99 dB	S11 = -13 dB	S11 = -10 dB	OrderN = 5	S11 = -15 dB	
$P_{\text{-1dB}}$	-18.3 dBm	NF = 2 dB	S22 = -10 dB	Max rej = 65 dB	S22 = -20 dB	
Sensitivity	-86 dBm	$P_{\text{-1dB}} = -7 \text{ dBm}$	S33 = -15 dB	ILoss = 2dB	NF = 13 dB	
Data rate	$3.2~\mathrm{Mbps}$	IIP3 = 3dBm	NF = 7 dB		IIP3 = 26 dBm	

DISCUSSION

Harmonic balance simulation results show that the simulated chirp spread spectrum FSK modulator output power spectral density meets FCC spectral mask requirement and the 500MHz bandwidth constrain. It is clear that the receiver performs frequency translation, filtering and amplification properly. More than 65 dB of side lobe rejection is achieved at receiver output. The simulation result shows a receiver output (Receiver_out) power range of -80 to -13.7 dBm/MHz which can drive the following sub band FSK demodulator stage.

The tuning range of the LPF enables suppression narrowband interferers and thus improves the interference rejection capability of the receiver.

The choice of non coherent versus coherent demodulation is a key system-level tradeoff. Although coherent demodulation can achieve very high transmission rates and better sensitivity than non coherent schemes, for low-data rate systems these benefits come at the cost of degraded energy efficiency. This is due to the power cost of precise timing synchronization hardware between transmitter and receiver which greatly increases the system complexity. Therefore, a non coherent dual band FSK demodulator based on energy detection can be used in this study.



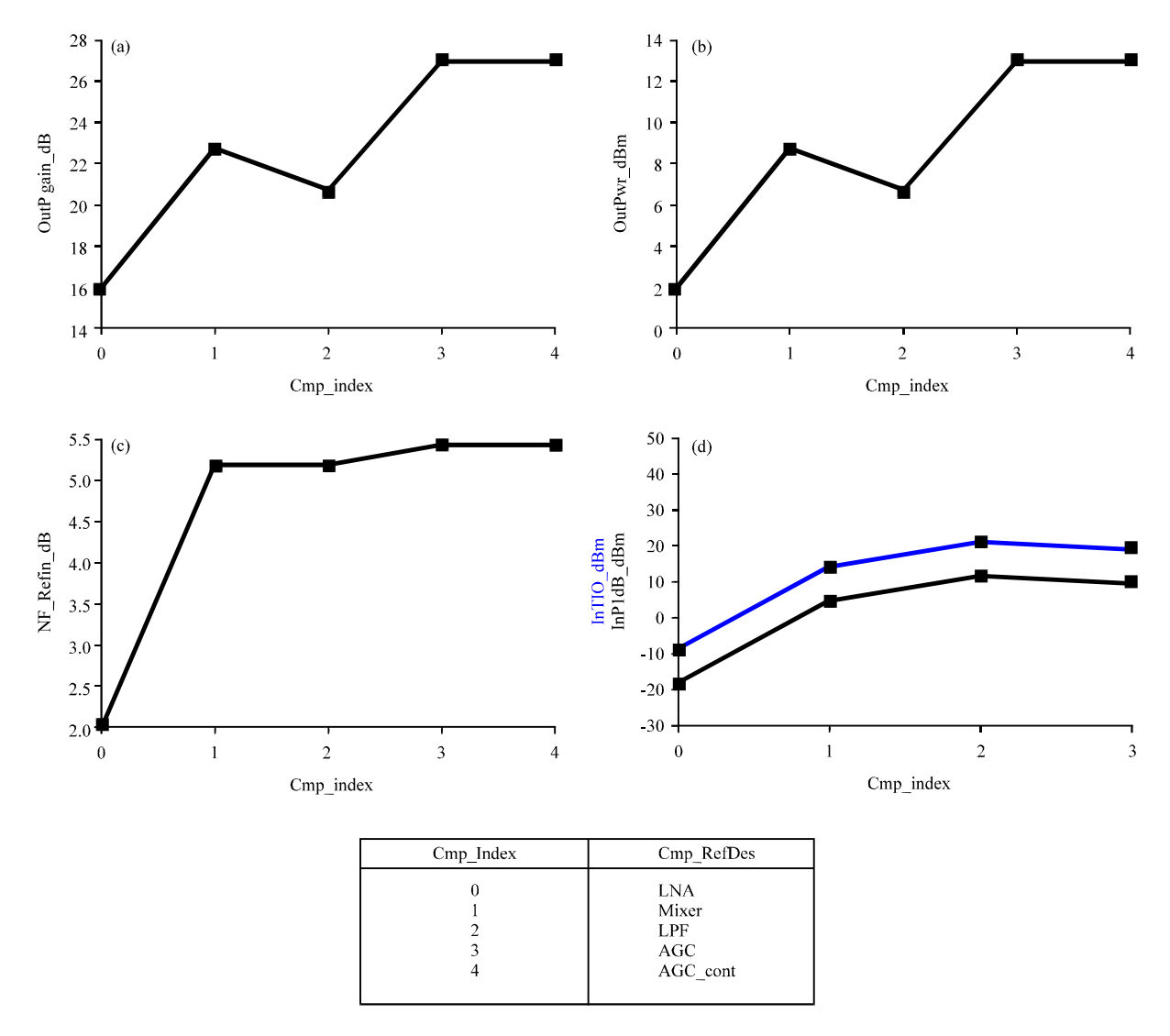


Fig. 7(a-d): (a) Simulated cascade voltage gain, (b) Cascade output power of the receiver, (c) Cascade noise figure and (d) Cascaded P_{.1dB} and IIP3, for Rx input power of -14 dBm

Chirped signal with FSK modulation enables direct conversion technique which simplifies the receiver architecture. The proposed receiver with direct conversion architecture and non coherent FSK demodulation technique relaxes center frequency tolerances, thus allowing for reduced hardware complexity. The center frequency may have drifted due to PVT variation. If a coherent demodulator is used at the receiver, the shift in center frequency can cause bit error due to timing synchronization between transmitter and receiver. A non coherent dual band FSK demodulator based on energy detection should be used in the receiver, where the amplitude information is more desired and the accuracy of pulse center frequency is less stringent. This technique relaxes center frequency tolerances, thus reducing bit error rate. The shift in center frequency could be tolerable in the proposed dual band FSK UWB receiver since it is much smaller than sub band width.

The benefits of the proposed UWB receiver for side lobe rejection have also been confirmed and the receiver can achieve more than 65 dB of side lobe rejection at the output.

Trends Applied Sci. Res., 9 (8): 461-471, 2014

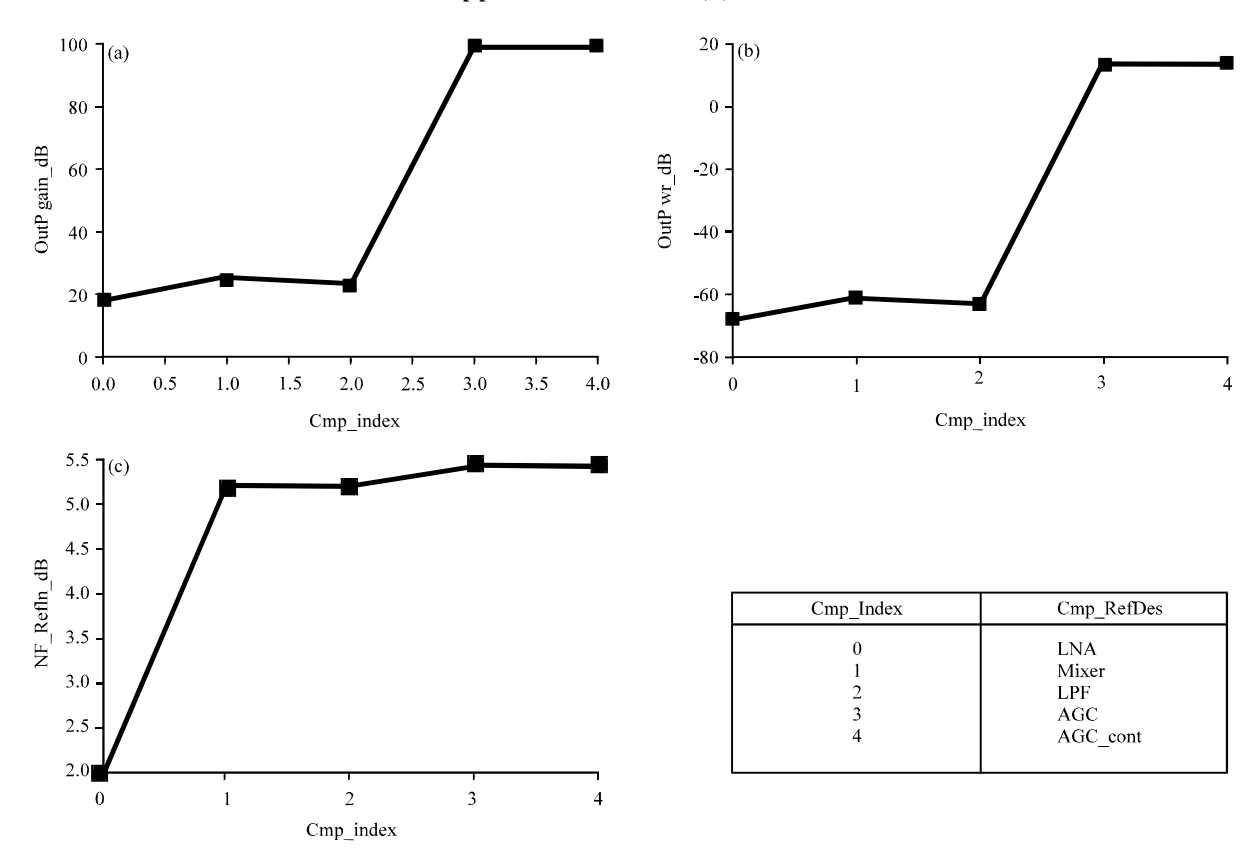


Fig. 8(a-c): (a) Simulated cascade voltage gain, (b) Cascade output power of the receiver, (c) Cascade noise figure, for Rx sensitivity power of -86 dBm

Table 2: Comparison with previously reported UWB receivers

	This study	Zheng et al. (2008)	Joo et al. (2010)
Modulation	Dual band FSK	BPM-BPSK	BPM-BPSK
Data rate	$3.2\mathrm{Mbps}$	$110~\mathrm{Kbps}$ to $31.2~\mathrm{Mbps}$	110Kbps/850 Kbps
Max pulse width	$75\mathrm{ns}$	$2\mathrm{ns}$	-
Max PSD	$-41.3~\mathrm{dBm/MHz}$	-	<-41.3 dBm/MHz
Sensitivity	$-86~\mathrm{dBm}$	-75 dB	$-79~\mathrm{dBm}$
Noise figure	5.4 dB	9.4 dB	$8.3~\mathrm{dBm}$
Gain	99 dB	90 dB	>90 dB
IIP3	-8.8 dBm	-12 dBm	-22 dBm

It is important to have variable bandwidth in order to suppress any in-band narrowband interferers from existing wireless technologies like Blutooth, Zigbee, 802.11 WLAN etc. In consequence the interference rejection capability of the receiver is improved and thus lowering the sensitivity of the receiver.

Simulation results show advantages in overall performance compared to conventional IR-UWB receiver topology. The receiver achieves a sensitivity of -86 dBm, a NF of 5.4 dB, an output power of 13dBm and an IIP3 of -8.8 dBm.

Table 2 summarizes the overall simulated performances of the receiver and presents a comparison with previously reported UWB receivers. The proposed design achieves better sensitivity, gain, IIP3 and noise figure than reported design by Zheng *et al.* (2008) and Joo *et al.* (2010).

CONCLUSION

A complete system architecture modeling, design and simulations for a short range, low data-rate and low complexity 3-5 GHz IR-UWB receiver front-end has been presented.

The UWB receiver utilizes a novel Chirped Spread Spectrum (CSS) dual-band FSK modulation scheme that circumvents the tradeoff between complexity and sensitivity that afflicts traditional architectures.

The receiver architecture adopts the direct conversion topology with non coherent FSK demodulation technique to target low power implementation.

The use of dual band FSK modulation within the transmitted pulses eliminates the pulse width and amplitude constraints faced by conventional IR-UWB. Furthermore, in the proposed receiver interference robustness is achieved by rejecting in-band interference using a variable bandwidth low pass filter after down conversion mixer.

Parameters for each block of the receiver chain are optimized so they meet the low power wireless sensor constraints. The results of this study validate chirped spread spectrum FSK IR-UWB receiver as a low-complexity, low data rate UWB radio technology which enable low power, short range healthcare wireless sensor application.

REFERENCES

- Abidi, A.A., G.J. Pottie and W.J. Kaiser, 2000. Power-conscious design of wireless circuits and systems. Proc. IEEE, 88: 1528-1545.
- Barras, D., F. Ellinger, H. Jackel and W. Hirt, 2006. A robust front-end architecture for low-power UWB radio transceivers. IEEE Trans. Microwave Theory Tech., 54: 1713-1723.
- Bilich, C.G., 2006. Bio-medical sensing using ultra wideband communications and radar technology: A feasibility study. Proceedings of the 1st International Conference on Pervasive Computing Technologies for Healthcare, November 29-December 1, 2006, Innsbruck, pp. 1-9.
- Culler, D., D. Estrin and M. Srivastava, 2004. Guest editors' introduction: Overview of sensor networks. Computer, 37: 41-49.
- Diao, S., Y. Zheng and C.H. Heng, 2009. A CMOS ultra low-power and highly efficient UWB-IR transmitter for WPAN applications. IEEE Trans. Circuits Syst. II: Express Briefs, 56: 200-204.
- IEEE, 2007. Part 15.4: Wireless Medium Access Control (MAC) and Physical Layer (PHY) Specifications for Low-Rate Wireless Personal Area Networks (LR-WPANs): Amendment to add alternate PHY. IEEE P802.15.4aTM/D7, January 2007, IEEE, New York, USA.
- Joo, S., W.H. Chen, T.Y. Choi, M.K. Oh, J.H. Park, J.Y. Kim and B. Jung, 2010. A fully integrated 802.15. 4a IR-UWB transceiver in 0.13 μm CMOS with digital RRC synthesis. Proceedings of the IEEE International Solid-State Circuits Conference, February 7-11, 2010, San Francisco, pp: 228-229.
- Lorincz, K., D.J. Malan, T.R.F. Fulford-Jones, A. Nawoj and A. Clavel *et al.*, 2004. Sensor networks for emergency response: Challenges and opportunities. IEEE Pervasive Comput., 3: 16-23.
- Padmanabhan, A., M. Sheplak, K.S. Breuer and M.A. Schmidt, 1997. Micromachined sensors for static and dynamic shear-stress measurements in aerodynamic flows. Proceedings of the International Conference on Solid State Sensors and Actuators, June 16-19, 1997, Chicago, IL., pp: 137-140.

Trends Applied Sci. Res., 9 (8): 461-471, 2014

- Paulson, C.N., J.T. Chang, C.E. Romero, J. Watson, F.J. Pearce and N. Levin, 2005. Ultra-wideband radar methods and techniques of medical sensing and imaging. Proceedings of the SPIE International Symposium on Optics East, October 23-26, 2005 Boston, MA., USA.
- Saputra, N. and J.R. Long, 2011. A fully-integrated, short-range, low data rate FM-UWB transmitter in 90 nm CMOS. IEEE J. Solid-state Circuits, 46: 1627-1635.
- Staderini, E.M., 2002. UWB radars in medicine. IEEE Aerosp. Electron. Syst. Mag., 17: 13-18.
- Zheng, Y., M.A. Arasu and K.W. Wong, 2008. A 0.18 μm CMOS 802.15.4a UWB transceiver for communication and localization. Proceedings of the IEEE International Solid State Circuits Conference, February 7-11, 2010, San Francisco, pp. 114-115.